Materials Research Proceedings 41 (2024) 641-650 https://doi.org/10.21741/9781644903131-71

Tool path strategies for single point incremental forming of fiber-reinforced thermoplastic sheets

RATH Jan-Erik Rath[1,a *] and SCHÜPPSTUHL Thorsten[1,b]

[1]Hamburg University of Technology, Institute of Aircraft Production Technology, Denickestr. 17, 21073 Hamburg, Germany

[a]jan-erik.rath@tuhh.de, [b]schueppstuhl@tuhh.de

Keywords: Composite, Fiber Reinforced Plastic, Incremental Sheet Forming, Tool Path

Abstract. Continuous fiber-reinforced thermoplastics (FRTP) are gaining increasing interest as a lightweight material. However, production processes such as thermoforming rely on costly molds, making them unsuitable for individual parts or small series production. Therefore, realizing an incremental sheet forming (ISF) process for FRTP is very desirable. As direct application of ISF to FRTP is impossible, researchers placed the FRTP between two metal sheets, allowing it to slide between them during single point incremental forming (SPIF). So far, only traditional tool path strategies for metal SPIF, such as the z-level or the spiral approach, have been used, which do not consider the draping requirements of woven reinforcement fibers. To optimize the forming process and prevent the development of wrinkles or other defects in the organo sheet, we propose and test novel tool path strategies for the SPIF of an FRTP sandwiched between two metal sheets. Results show that the proposed strategies have a positive impact on part quality, as fiber orientation-based tool path approaches show less wrinkling and higher part accuracy in SPIF without support.

Introduction

Fiber-reinforced plastic (FRP) composites are increasingly popular due to their high strength-to-weight ratios and other properties. Among the reinforcement materials, woven fibers are frequently used because of their comparably high reinforcing effect, good handling and draping properties, and wide availability [1,2]. In recent years, the somewhat contrary demands for efficiency and flexibility of FRP production processes have increasingly been addressed by automation and robotics, especially in additive processes such as Automated Fiber Placement (AFP), robotic layup, or 3D printing [3]. Still, the hand-layup process, manually draping fiber fabrics on a mold and subsequently impregnating them with a thermoset resin, is commonly used for prototype and small series production [4]. However, fiber-reinforced thermoplastics (FRTP) are gaining more and more relevance in the market due to their superior ductility, damping properties, corrosion resistance, weldability, and reshapeability, among others [1]. As a result of the high viscosity of thermoplastic matrices, pre-impregnated and consolidated flat sheets, called organo sheets, are commonly used as a semi-finished product and formed in thermoforming processes involving at least one part-specific mold. Due to the high cost and effort to produce, maintain, and store these molds, an economical production process for prototypes and small series using organo sheets is missing [5].

One solution to this problem could be incremental sheet forming (ISF), where a metal sheet is clamped on its edges and locally deformed with a standard tool, such as a hemispherical tooltip, guided by a CNC machine or an industrial robot. In addition to single point incremental forming (SPIF), process variations, including a die or a supporting tool on the other side of the sheet, exist [6]. While the ISF of thermoplastics has been demonstrated [7], its direct application to FRTP, especially with continuous fibers, is not readily possible. While metal and thermoplastic sheets deform by stretching and thinning, the continuous fibers would break when clamped on the edges [8]. Therefore, researchers incrementally formed the FRPs together with at least one metal dummy sheet, allowing the fibers to slide relative to it. Fiorotto et al. [9] used a vacuum bag to apply a

woven thermoset prepreg to a metal sheet, protecting the FRP surface and transferring the deformation to the flexible fabric. Xiao et al. [10] and Xu et al. [11] placed a die below the sheet layup in a two-point incremental forming process. Heated continuous fiber-reinforced organo sheets were formed between two metal dummy sheets with PTFE layers to reduce adhesion, by Al-Obaidi et al. [5,12], Emami et al. [13], and Hou et al. [8]. Conte et al. [14] proposed to use the pressure of a heated fluid to apply an FRTP onto a metal sheet during SPIF. Defects such as cracks and wrinkles were often observed, especially at higher wall angles [5,8,13]. One reason could be the tool path strategies used, which have been basic z-level or spiral contouring tool paths of metal SPIF. Hou et al. [8] were the only researchers to additionally try an inside-out tool path, starting forming in the center of the sheet in each layer, and reported on improved part quality.

While the standard tool path strategies have been proven for metal sheets, they do not account for the deformation mechanisms of woven fiber fabrics, which must be sheared to represent a 3D shape with double curvature smoothly. This shear is usually introduced by tensioning the fabric in-plane in fiber or bias direction [4], which is hard to realize with undetermined fiber movement between two metal sheets and in a dieless process. Therefore, Rath et al. [15] developed a draping strategy for the dieless forming of woven FRP and tested it in various alternative processes for forming FRP without a mold [16,17]. The strategy involves a 3D tool movement in fiber direction along the target geometry, starting at a fixed point and moving towards the edge of the fabric. As the sequence of the paths is determined according to an ascending shear angle in the fabric as projected by a simulation, shear is introduced in a determined manner.

This paper aims to adapt the draping strategy [15] to SPIF to improve the incremental forming of woven FRPs together with metal dummy sheets. Therefore, multiple novel tool path strategies taking into account both the requirements of metal forming and fabric draping are developed and tested in a setup very similar to the one realized by Al-Obaidi et al. [5,12].

Methodology

Materials. For each forming experiment, a woven carbon fiber-reinforced organo sheet was placed between two metal sheets, separated on each side by PTFE sheets to allow the sliding of the CFRP. The fiber orientations corresponded to the edges of the sheets and were therefore also aligned with the clamping frame. The organo sheets consisted of a styrene-acrylonitrile (SAN) matrix and two layers of twill-woven carbon fibers (CF) with a basis weight of 245 g/m², resulting in a thickness of 0.6 mm and a fiber-volume content of 45 %. With a size of 210 mm x 240 mm, the CFRP was smaller than the metal sheets with 350 mm x 350 mm. On the lower side, an aluminum sheet EN AW-1050A with a thickness of 0.5 mm was used as a backing plate. On the upper side, a DC04 steel sheet of 0.8 mm thickness was used to transfer the deformation while protecting the organo sheet from direct tool contact. The PTFE sheets were of 0.05 mm thickness and 270 mm x 270 mm in size. The layup is shown in Fig. 1.

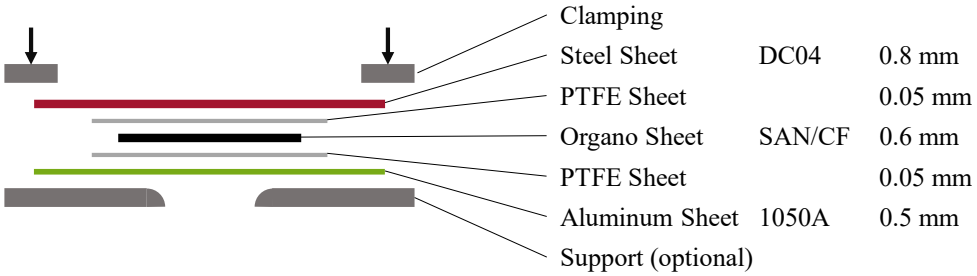

Fig. 1 Layup of organo sheet, PTFE sheets, and metal sheets, including clamping and support

Setup. The sandwich layup of metal, PTFE, and organo sheets was clamped on top of a heating chamber made of vermiculite and calcium silicate panels. It was ensured that only the metal sheets

were clamped while the organo and PTFE sheets could slide between them. Due to the comparatively high distance between the formed area and the clamping, for some experiments, a rigid support plate with 5 mm thickness and a hole of 105 mm diameter with 5 mm edge radius was additionally placed below the aluminum sheet to act as a template, as shown in Fig. 1. Two Leister Mistral 2 Premium hot air guns, each with a power of 3.4 kW, were used to heat the layup to 180-200 °C. Thereby, the hot air was deflected downwards, as this resulted in a homogeneous temperature distribution on the sheet stack in initial tests. Temperature was measured on the top steel sheet using two thermocouples. The clamping was tightened only after the desired temperature was reached to allow thermal expansion of the metal. SPIF was performed using a steel 1.2210 tool with a hemispherical tip of 20 mm diameter guided by an ABB IRB 6660-205 industrial robot with 205 kg load capacity, as shown in Fig. 2.

After forming, the layup was cooled to room temperature, unclamped, and separated. The resulting geometries were visually inspected for defects such as cracks or wrinkles and 3D-scanned with a GOM ATOS CompactScan 5M.

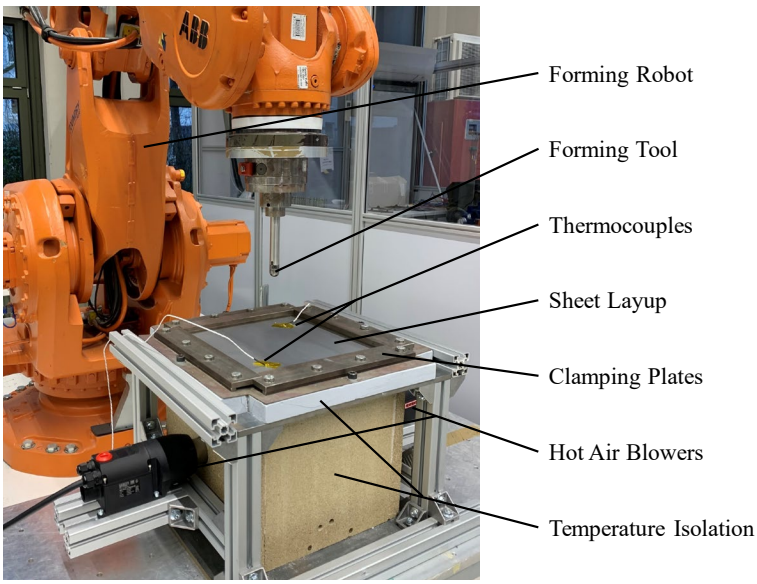

Fig. 2 Robotic single point incremental forming setup with heating chamber

Forming Strategies. Frustum cones with an upper diameter of 100 mm, a lower diameter of 25 mm, and a height of 30 mm were formed, corresponding to a wall angle of approx. 38.7°. Unless stated otherwise, a tool speed of 20 mm/s and a layer height of 0.5 mm was used. The tool orientation was kept constant throughout the process, and no lubrication was used.

First, a traditional z-level contouring strategy was used as a reference, denoted as strategy 1. Thereby, the tool travels along the outer contour of the cone in each layer, stepping down after each circle. The same is done in strategy 2, except that at the end, the lower face of the truncated cone is filled spirally from the outside to the inside, radially moving inwards 0.6 mm with every revolution. In strategy 3, each layer is formed by spiraling from the center point to the outer contour, filling each slice, again with a winding pitch of 0.6 mm.

Strategy 4 aims to resemble the path forming strategy for fabric draping developed by Rath et al. [15]. However, because forming in SPIF must originate from the initial plane, it is not possible to follow 3D paths directly. Instead, the paths running from a central starting point outwards along the fiber orientations of the fabric are projected in the cutting planes of the geometry. Therefore, just like strategy 3, strategy 4 also includes slicing the desired geometry and filling each layer with tool paths; however, the orientation of these paths depends on the fiber orientations of the woven

fabric and their sequence on the projected shear angle. First, straight lines are formed from the center point outwards in four perpendicular directions, corresponding to the directions of the perpendicular warp and weft yarns of the fabric. Subsequently, parallel paths are formed on both sides of the four lines, again traveling from the inside to the outside, maintaining a distance of 2 mm between the already created lines. This process is repeated until the whole contour of the layer is filled with parallel lines. After completing a layer, the next z-increment of 0.75 mm is formed likewise, again starting from the center point. Tool speed during the forming operations was 20 mm/s and higher during transfer movements of the robot to reach the starting point of the following path when the tool was out of contact with the surface.

In strategies 1 to 4, forming starts with the upper, larger diameter, which requires the fabric to always slide inwards through the cone's already created edge and slope. However, it would be better and more closely match the draping strategy if the cone was formed starting with the lower, smaller diameter. This approach, however, would require moving the whole already formed geometry downwards and adding on to the slope until reaching the upper diameter. As a controlled rigid body movement is hard to achieve in SPIF, the already formed geometry must be pushed downwards at every point to realize the desired deformation. This ought to be achieved with strategy 5, which incorporates actual 3D paths. First, parallel paths in perpendicular fiber directions are formed at the first z-level, just as in strategy 4; however, only up to the diameter of the lower face of the cone. Subsequently, these paths are repeated at the next z-level, whereby they are extended along the lateral surface slope until the radius of the next slice is reached at z = 0. This process is repeated until the desired height is achieved, again with a z-increment of 0.75 mm.

Fig. 3 gives an overview of the different forming strategies. For better visibility of the paths, a higher winding pitch, path distance, and z-increment were used in the plots, and layers were additionally separated.

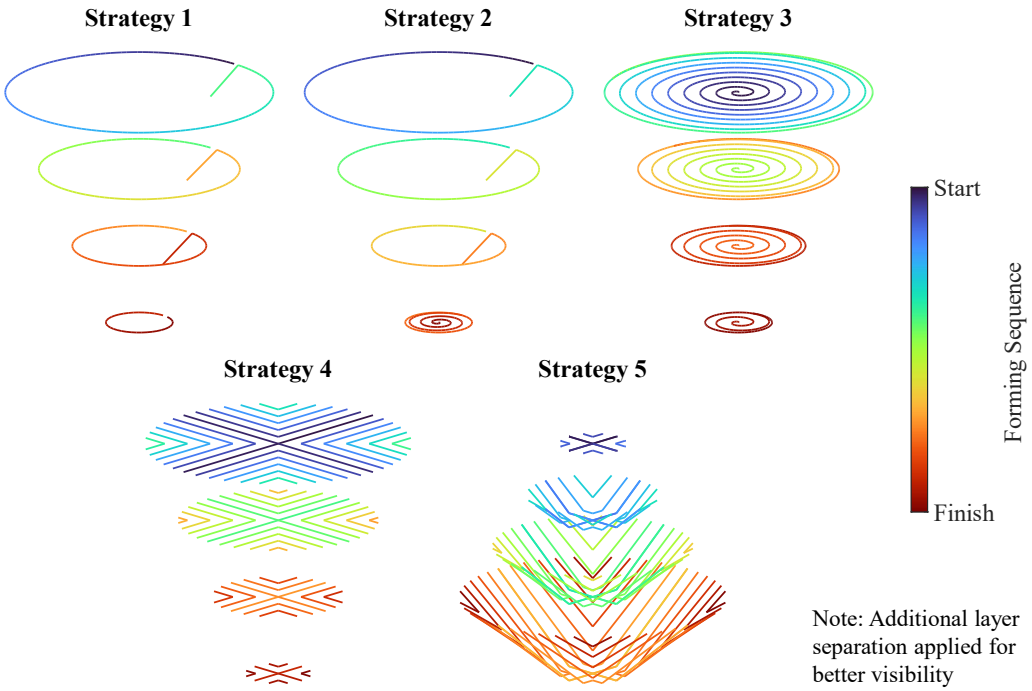

Fig. 3 Overview of the tool path strategies used for SPIF of woven FRPT sheets

Results & Discussion

Visual Observations. Fig. 4 shows all organo sheets that were formed into conical shapes. None of these developed any macroscopic cracks. As desired, fibers were drawn in towards the forming

area and bent successfully. However, the amount of shear achieved in the fabric differs significantly among the strategies. The results of strategies 1 and 2 without support show wrinkles of high magnitude, especially in the corners, where the woven fabric should have been sheared. Towards the more advanced strategies, more shear becomes visible, and wrinkles decrease in height while increasing in width. Among the experiments without support, strategy 5 introduced the most shear and produced the smoothest and most distinguishable cone with a clearly visible base edge. This result, however, is the case for all experiments with support. While all eventual wrinkles are minor in height compared to forming without support, strategies 1 and 2 show more small wrinkles in the material surrounding the cone, which would be trimmed in practice.

On all organo sheets, deconsolidated areas are visible, where the surface shows the individual yarns instead of a smooth matrix layer. In strategies 3 and 4, this effect leaves most of the cone's surface, except for the lower part, uncovered. This might not only be due to resin accumulation because of gravity but also to the formation of a gap between the metal sheets. Comparing strategies 1 and 2, the effect of forming and thus applying pressure on the composite becomes visible. As the bottom surface of the cone was not covered by paths in strategy 1, no pressure was applied, and the organo sheet deconsolidated. The same happened on the lateral surface areas of cones formed in strategies 1 and 2 with support, where the lower aluminum sheet cracked and tore during the process, as visible in Fig. 5, thus not providing support for consolidation. A reason for the tearing could be that the commonly used contour tool paths in strategies 1 and 2 provoke rigid body motion of the area enclosed by the contour, leading to a more widely distributed pressure on the aluminum sheet instead of a relatively localized force in the other strategies. With the support preventing a global deformation of the aluminum sheet, cracks developed, and the sheets tore.

As shown in Fig. 5, cracks also appeared in both upper and lower metal sheets used in strategy 5. As the primary deformation occurs in the bottom surface of the cone, which is pushed downwards layer by layer, material thinning led to the development of cracks in the steel sheet starting at nominal depths of 28.5 mm and 23.5 mm without and with support, respectively. These cracks in the path direction grew with increasing depth and, in the case of the experiment with a support plate, led to the formation of tears perpendicular to the path direction, forcing the termination of the forming process at a depth of 26.25 mm. Without support, the sheets bent and deformed more globally in the free area within the clamping frame. Therefore, the actual depth of the cone with respect to the base plate was lower than the nominal depth of the tool and forming was possible until the end.

Unlike the other strategies, both results from strategy 5 show a spreading of the yarns in the formed area. This effect intensifies towards the bottom surface of the cone and must be due to a high and repeated compaction of the yarns under pressure from the tool. Another observation for strategy 5 that is more noticeable when support is used is that the base of the cone is no longer circular. Particularly towards the end of the forming process, the tool is deflected from the diagonals formed by the starting points of the paths on the lateral surface of the cone, towards the initial, central paths. As a result, the paths are no longer perpendicular to each other, as highlighted in Fig. 5, and the radius of the base circle decreases towards the diagonals. The reason for this result is that the paths in strategy 5, except the initial paths starting from the center, do not run radially but combined radially and tangentially along the lateral surface of the cone. However, the resistance to the deformation acts, in simple terms, normal to the surface so that a force component perpendicular to the direction of movement results. This force is higher in case the support is used, and the comparatively low stiffness of the robot thus causes a deviation from the target paths.

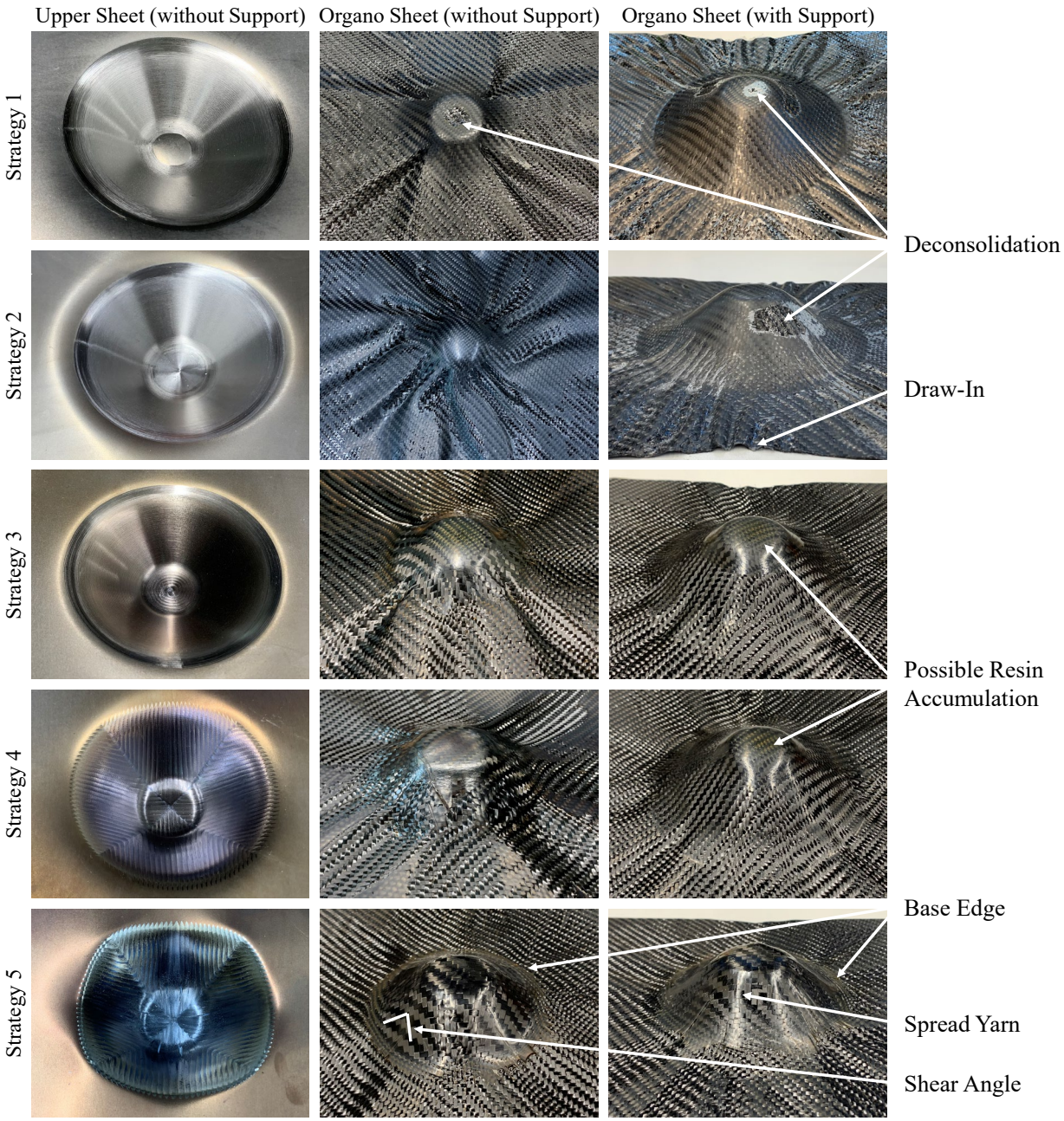

Fig. 4 Upper steel sheets formed without support (view on cone facing down), as well as formed organo sheets for all path strategies with and without support (view on cone facing up)

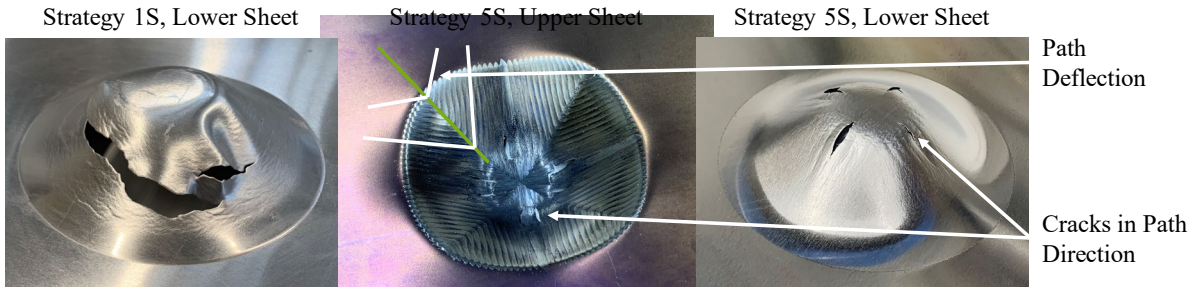

Fig. 5 Cracks in the lower aluminum and upper steel sheets after forming with support (S)

3D Scans. Optical 3D measurements of the formed sheets allow for a quantitative evaluation and comparison of the results. For this purpose, each scanned point cloud was meshed before an ideal target cone surface was manually aligned and then fine-registered with it using the Iterative Closest Point Algorithm (ICP). In accordance with the target geometry, the scanned surface was segmented at a radial distance of 20 mm around the upper base circle edge of the cone. Finally, absolute and signed distances between the scanned and the target meshes were calculated. The results are shown in Fig. 6, in top view on the upwards-facing cone.

All cones formed without support are below the target geometry in the tip area, denoted by blue color, and generally above the target geometry around the base circle, indicated by red color. This means that the desired height of the cones could not be reached. Furthermore, the wrinkles are clearly visible in the images. However, among the experiments without support, an improvement in shape accuracy can be observed for each more sophisticated strategy. This is also reflected in the mean absolute distances, plotted in Fig. 7, and matches the visual observations from above. Strategy 5, which builds the cone in a tip-to-base approach best corresponding to the draping requirements of woven fibers, especially sets itself apart. In every formed layer, the tool movements along the fiber directions compact the fabric, push eventual wrinkles outwards through the lateral surface of the cone, and foster the introduction of shear through pulling in fiber direction.

However, an even better match between the samples deformed with support and the target geometry becomes evident from the results, even though the color scales are different to better visualize the localization of the distances on the surfaces. Among the samples deformed with support, the mean absolute distances are very similar except for strategy 5, where the cone did not reach the target height for the abovementioned reasons. Furthermore, the frequent loading and unloading of the sheet by detaching and repositioning the tool in strategies 4 and 5 could have led to unfavorable sliding of the sheets over the edge of the support, which also would have had to grow with the current base circle diameter for strategy 5 to fully unfold its advantages.

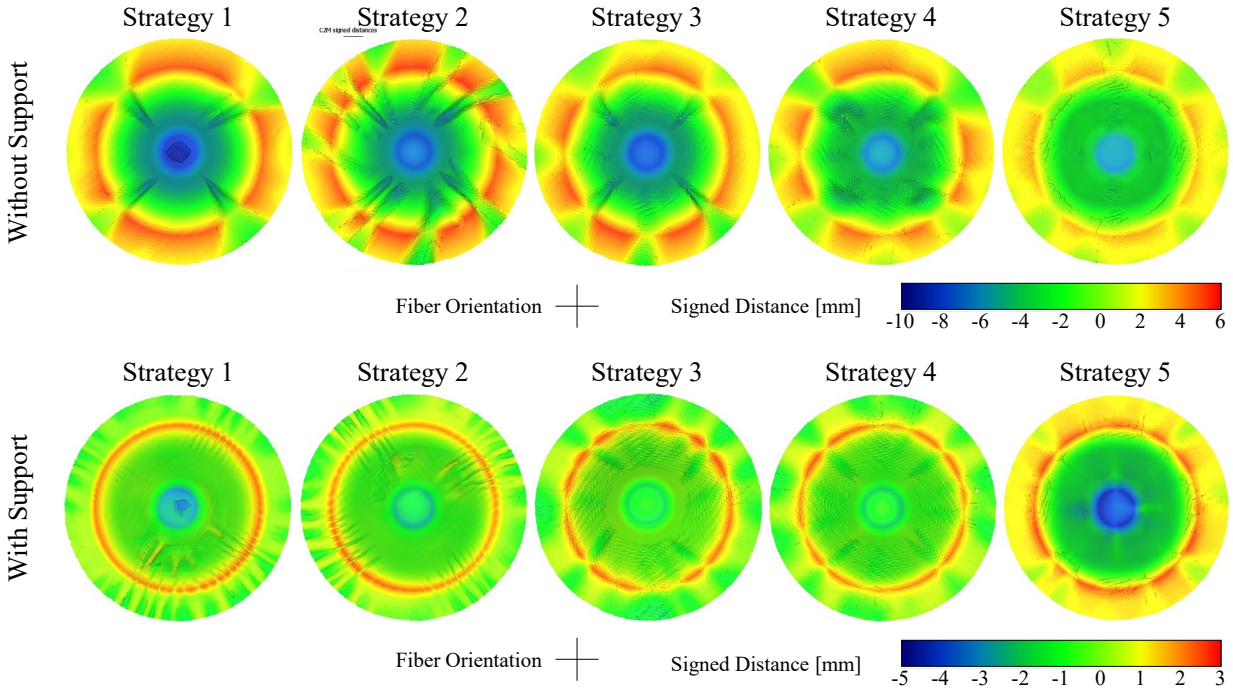

Fig. 6 3D Scans of organo sheets formed without and with support, colors represent signed distances to target geometry (please note different scales)

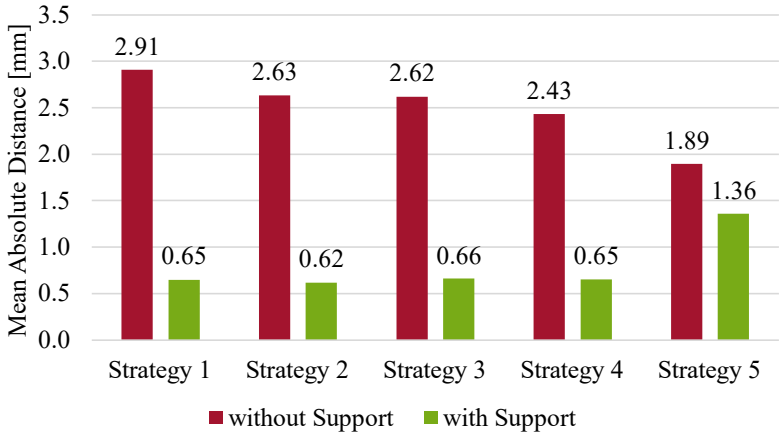

Fig. 7 Mean absolute distances between formed organo sheets and target geometry

Cross Sections. The reason for the better shape accuracy of cones formed with support becomes apparent when looking at Fig. 8, showing a comparison of cross sections of the scanned surfaces of the upper steel sheets, organo sheets, and lower aluminum sheets on the example of strategy 4 experiments with and without support. As mentioned above, the unsupported deformation of the sheets includes a global elastic and plastic bending, which is significantly more pronounced for the lower aluminum sheet than for the upper steel sheet. While the tool introduces a relatively local deformation in the upper sheet, forming forces are transferred and spread within the steel, PTFE, and organo sheets, so that the pressure on the aluminum sheet is applied in a comparably more extensive area, leading to a rather global deformation. As the two metal sheets detach and voids build between them, the enclosed organo sheet obtains space for the development of wrinkles and, due to gravity, conforms to the lower, globally bent sheet. In contrast, if the lower sheet is supported, the geometries of all three sheets match relatively well, apart from deviations caused by elastic spring-back and other effects.

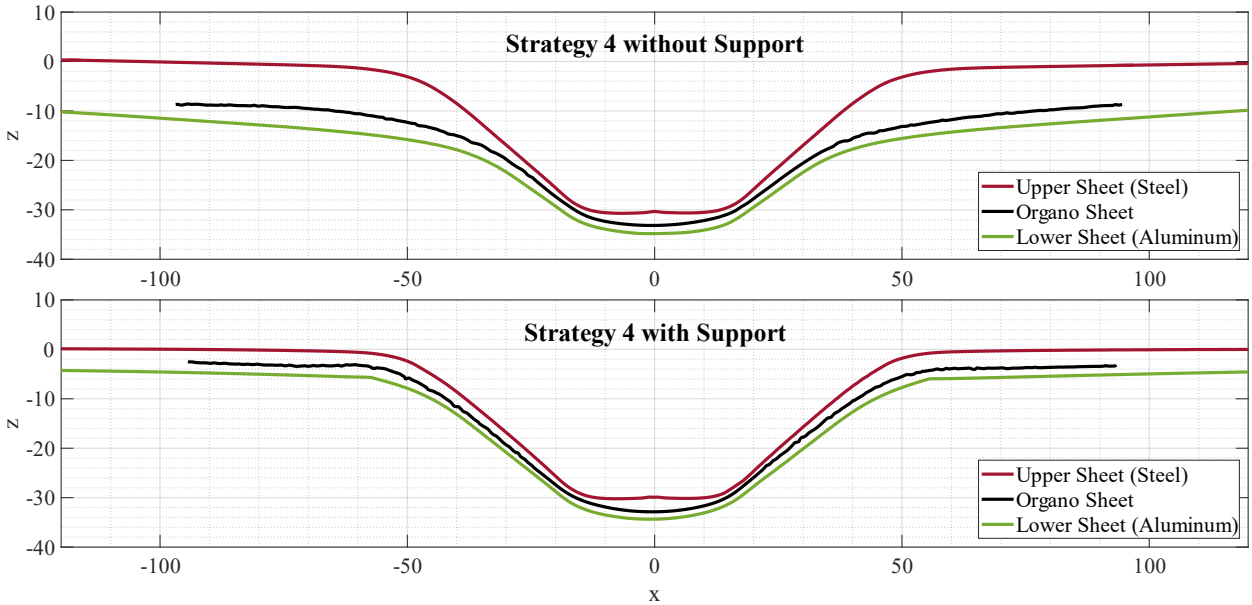

Fig. 8 Comparison of cross sections of formed sheets for strategy 4 without and with support, each taken through the center of the cone and manually aligned in x-z-plane for comparison

Summary, Conclusions & Outlook

Combining the flexibility of a robot with a digital process chain in a dieless forming process, robotic ISF can open new opportunities for the economic production of FRP prototypes and individual parts. In order to optimize part accuracy and quality in SPIF of woven FRP placed between two metal sheets, different novel tool path strategies were developed, tested, and compared to a conventional contouring strategy. These include surface-filling z-level approaches, such as spiraling inside out or moving in parallel lines in the fiber directions in each slice, and a three-dimensional approach inspired by fabric draping. From the results, it can be concluded that tool paths considering the draping requirements of woven FRP can lead to better results in SPIF without support. Paths following the fiber directions apply tension in the underlying fabric in fiber direction, introducing the necessary shear. Forming the cones in a tip-to-base approach with 3D tool paths yielded the best results in unsupported SPIF. However, as the already formed area of the cone needs to be pushed downwards in every subsequent step and paths are repeatedly formed on each z-level, a higher metal sheet thickness is required to prevent the development of cracks.

An even more significant improvement in part accuracy was achieved by introducing a fixed support with the size of the cone's base diameter below the sheets, preventing global bending of the lower metal sheet due to a spreading of the forming force through the layers. However, using conventional tool paths, the lower sheet tore in the supported setup, which led to the local deconsolidation of the FRTP due to the lack of pressure being applied on the organo sheet. The improved tool path strategies prevented the tearing while not entirely preventing deconsolidation—instead, the thermoplastic matrix accumulated in the lower part of the cone.

Further experiments with different metal and organo sheet configurations and forming temperatures should be conducted to investigate their influence on part quality, taking into account microscopic analyses to determine resulting consolidation states, fiber-volume-contents, and internal defects. Forming limits for the individual strategies need to be determined by forming different geometries, varying wall angles. In addition, investigations on other fiber architectures and textiles, such as triaxial woven fabrics or non-crimp fabrics (NCF) would be of relevance. Specifically, it should be studied if fiber orientation-based tool path approaches are also applicable and beneficial in these cases, which is expected by the authors. Simulations of the thermo-mechanical deformation and draping behavior of the fabrics should be used to determine the shear angles and the fiber deflections from the initial state as inputs to the path planning. Lastly, an optimized support, such as a globally applied hydrostatic pressure or even a double-sided incremental forming process, should be tested in conjunction with the optimal tool path strategy.

References

[1] M. Neitzel, P. Mitschang, U. Breuer, Handbuch Verbundwerkstoffe: Werkstoffe, Verarbeitung, Anwendung, 2nd ed., Hanser, München, 2014.

[2] K. Bilisik, N.S. Karaduman, N.E. Bilisik, Fiber Architectures for Composite Applications, in: R. Fangueiro, S. Rana (Eds.), Fibrous and Textile Materials for Composite Applications, 1st ed., Springer Singapore, Singapore, 2016, pp. 75–134.

[3] P. Boisse, R. Akkerman, P. Carlone, L. Kärger, S.V. Lomov, J.A. Sherwood, Advances in composite forming through 25 years of ESAFORM, Int J Mater Form 15 (2022). https://doi.org/10.1007/s12289-022-01682-8

[4] S.G. Hancock, K.D. Potter, The use of kinematic drape modelling to inform the hand lay-up of complex composite components using woven reinforcements, Compos. - A: Appl. Sci. Manuf. 37 (2006) 413–422. https://doi.org/10.1016/j.compositesa.2005.05.044

[5] A. Al-Obaidi, A. Kunke, V. Kräusel, Hot single-point incremental forming of glass-fiber-reinforced polymer (PA6GF47) supported by hot air, J. Manuf. Process. 43 (2019) 17–25. https://doi.org/10.1016/j.jmapro.2019.04.036

[6] L. Ben Said, The incremental sheet forming; technology, modeling and formability: A brief review, Proc. Inst. Mech. Eng. E: J. Process Mech. Eng. 236 (2022) 2729–2755. https://doi.org/10.1177/09544089221093306

[7] P. Martins, L. Kwiatkowski, V. Franzen, A.E. Tekkaya, M. Kleiner, Single point incremental forming of polymers, CIRP Annals 58 (2009) 229–232. https://doi.org/10.1016/j.cirp.2009.03.095

[8] C. Hou, X. Su, X. Peng, X. Wu, D. Yang, Thermal-Assisted Single Point Incremental Forming of Jute Fabric Reinforced Poly(lactic acid) Biocomposites, Fibers Polym. 21 (2020) 2373–2379. https://doi.org/10.1007/s12221-020-1016-0

[9] M. Fiorotto, M. Sorgente, G. Lucchetta, Preliminary studies on single point incremental forming for composite materials, Int. J. Mater. Form. 3 (2010) 951–954. https://doi.org/10.1007/s12289-010-0926-6

[10] X. Xiao, J.-J. Kim, S.-H. Oh, Y.-S. Kim, Study on the incremental sheet forming of CFRP sheet, Compos. - A: Appl. Sci. Manuf. 141 (2021) 106209. https://doi.org/10.1016/j.compositesa.2020.106209

[11] P. Xu, X. Li, F. Feng, X. Li, Y. Yang, Experimental and numerical studies on two-point incremental forming of woven fabric composite sheet, J. Manuf. Process. 85 (2023) 205–215. https://doi.org/10.1016/j.jmapro.2022.11.049

[12] A. Al-Obaidi, A. Graf, V. Kräusel, M. Trautmann, Heat supported single point incremental forming of hybrid laminates for orthopedic applications, Procedia Manuf. 29 (2019) 21–27. https://doi.org/10.1016/j.promfg.2019.02.101

[13] R. Emami, M.J. Mirnia, M. Elyasi, A. Zolfaghari, An experimental investigation into single point incremental forming of glass fiber-reinforced polyamide sheet with different fiber orientations and volume fractions at elevated temperatures, J. Thermoplast. Compos. Mater. 36 (2022) 1893-1917. https://doi.org/10.1177/08927057221074266

[14] R. Conte, G. Serratore, G. Ambrogio, F. Gagliardi, Numerical analyses of long fiber–reinforced polymeric sheets processed by Single Point Incremental Forming, Int. J. Adv. Manuf. Technol. 123 (2022) 1203–1214. https://doi.org/10.1007/s00170-022-10212-4

[15] J.-E. Rath, L.-S. Schwieger, T. Schüppstuhl, Robotic Die-Less Forming Strategy for Fiber-Reinforced Plastic Composites Production, Procedia CIRP 107 (2022) 1281–1286. https://doi.org/10.1016/j.procir.2022.05.145

[16] J.-E. Rath, R. Graupner, T. Schüppstuhl, Processing Strategies for Dieless Forming of Fiber-Reinforced Plastic Composites, Machines 11 (2023) 365. https://doi.org/10.3390/machines11030365

[17] J.-E. Rath, T. Schüppstuhl, Investigation of Metal Wire Mesh as Support Material for Dieless Forming of Woven Reinforcement Textiles, JMMP 7 (2023) 182. https://doi.org/10.3390/jmmp7050182